water

MDPI

Article

Action of Low-Density Polyethylene Microspheres in the Transport of Metformin Hydrochloride in Aqueous Medium Through Adsorption and Desorption

Luanna Gláucia Guimarães, Renata Medici Frayne Cuba and Francisco Javier Cuba Teran *

School of Civil and Environmental Engineering, Federal University of Goias, Goiania 74605-220, Brazil; guimaraesluanna@discente.ufg.br (L.G.G.); renatafrayne@ufg.br (R.M.F.C.)
* Correspondence: paco@ufg.br

Abstract: The present study addresses the issue of transporting pharmaceuticals via microplastics in aquatic environments. For this purpose, the adsorption and desorption of metformin hydrochloride (MET), a hydrophilic compound, on polyethylene microspheres (PMEs) were studied via batch adsorption and desorption capacity and kinetics tests. The adsorption test results indicated minimal influence of pH values above 5, alongside a decrease in adsorption capacity with an increasing mass of PMEs. The Freundlich model best represented the adsorption capacity data; however, values of $n < 1$ (0.6) and low K suggest a decrease in the sorption affinity of MET with increasing initial MET concentration and a low affinity of MET for PM beads. The rate and equilibrium of adsorption were fast, and the results adequately fit the pseudo-first- and pseudo-second-order models, suggesting that physical and chemical mechanisms contributed to the adsorption of MET onto the PEMs under the conditions of this study. The desorption equilibrium result was 1.3 mg $g^{-1} \pm 0.04$ mg g^{-1}, without significant change, regardless of the initial amount of adsorbed MET. However, the desorption percentage varied between 26.14% and 7.01% as a function of the amount. of MET adsorbed onto the PMEs. These results suggest that PMEs could be potential vectors of MET transport in aquatic environments.

Keywords: microplastic; pharmaceutical products; water pollution; contaminant vectors

Citation: Guimarães, L.G.; Cuba, R.M.F.; Teran, F.J.C. Action of Low-Density Polyethylene Microspheres in the Transport of Metformin Hydrochloride in Aqueous Medium Through Adsorption and Desorption. *Water* **2024**, *16*, 3332. https://doi.org/10.3390/w16223332

Academic Editors: António Manuel Abreu Freire Diogo, Enedir Ghisi and Célia dos Anjos Alves

Received: 2 October 2024
Revised: 14 November 2024
Accepted: 17 November 2024
Published: 20 November 2024

1. Introduction

Plastics are composed of high-molecular-weight synthetic organic polymers whose physicochemical characteristics, such as strength, lightness and durability combined with low manufacturing costs, make them essential materials for economic expansion, innovation, and production of low-priced goods in the world market, particularly in emerging markets where industry continues to grow [1].

As a result, the global production of plastics increased from approximately 245 million metric tons in 2008 to 359 million metric tons in 2018, and this value is expected to triple by the year 2050 [2].

Owing to the extensive use of plastic-based products coupled with their low recycling and reuse rates, residues of these materials are released in a generalized way in different environmental compartments especially in aquatic systems [3].

The plastic wastes commonly detected in aquatic environments are some of the most produced and used in anthropic activities. These include polyethylene (PE), polyvinyl chloride (PVC), polypropylene (PP), polyethylene terephthalate (PET) and polystyrene (PS) [4].

Plastic waste of different sizes is found in water resources, but particles with sizes between 1 nm and 5 mm, defined as microplastics (MPs) [5], have been recognized as one of the most complex environmental problems today, both because of their abundance and their effects on ecosystems [6].

MPs are classified as primary when they are microsized, usually used in cosmetics and beauty products [7], and secondary when they are generated from plastic waste present in the environment which undergoes continuous fragmentation caused by a combination of mechanisms that include photodegradation by ultraviolet (UV) radiation, mechanical abrasion, chemical, biological and thermal degradation and disintegration [8].

One of the main sources of MPs is wastewater, and although sewage treatment plants (ETEs) usually achieve removal of more than 95% of MPs [9], a significant number of particles still enter the environment through effluent discharge [10]. Furthermore, the MPs removed by ETEs is transferred to sludge, which, when applied to agricultural lands as biosolids, can also reach the aquatic environment via surface runoff [11].

Owing to their small size and slow biodegradation rate, MPs can be easily absorbed and bioaccumulated by organisms [12], resulting in various deleterious effects on their survival, physical fitness, metabolism, growth and reproduction [3].

In addition, characteristics such as hydrophobicity, a high surface area-to-volume ratio, high stability and mobility give MPs a strong tendency to adsorb and enrich hydrophobic organic compounds (HOCs) [13] and metals. The hypothesis that MP particles may act as transport vectors of pollutants and microorganisms between different environmental compartments has been proposed [14].

The distribution of contaminants between MPs and the aqueous phase is a function of their intrinsic properties and environmental conditions, including the presence of interfering compounds in the process. Atugoda et al. [15] reported that, owing to the high surface area of MPs, the amount of contaminants that accumulate on the surface of these materials can reach several orders of magnitude greater than that in the surrounding waters.

Among the compounds capable of adsorbing to MPs under various conditions, pharmaceuticals, including endocrine disruptors, are of great environmental interest because of their deleterious effects on ecosystems and human health [16]. However, owing to the hydrophobic characteristics of MPs, studies involving the adsorption/desorption of hydrophilic compounds are scarce, thus reflecting the lack of information on the different interaction mechanisms involved in these processes.

Among such hydrophilic compounds, metformin, which is the main drug used to treat type 2 diabetes mellitus, as well as COVID-19 and polycystic ovary syndrome, has seen a considerable increase in consumption [17].

The presence of metformin has already been detected in sanitary sewage, effluents from sewage treatment plants and even in aquatic environments. Mayoudom et al. [18] detected the presence of 19 drugs and/or their metabolites in the sewage of the University Teaching Hospital of Yaoundé (UTHY), with metformin having the second highest concentration (154 $\mu g\ L^{-1}$), second only to paracetamol (211.9 $\mu g\ L^{-1}$). In Germany, Trautwein et al. [18] identified the presence of metformin at multiple points in fresh and saltwater and domestic sewage, with the maximum values obtained in raw domestic sewage (142.3 $\mu g\ L^{-1}$), WWTP effluent (67.2 $\mu g\ L^{-1}$), lakes (216 $ng\ L^{-1}$), river water (645 $ng\ L^{-1}$) and seawater (463 $\mu g\ L^{-1}$).

Even at low concentrations, such as those detected by Souza et al. [19], metformin can cause behavioral and physical changes in fish, such as altered mitochondrial metabolism, stress behaviors and even mortality.

Despite its relevance, the interaction between metformin and microplastics is a phenomenon that has rarely been studied to date; therefore, the present study aims to evaluate the behavior of polyethylene microspheres with respect to the transport of metformin hydrochloride in aqueous media by adsorption and desorption.

2. Materials and Methods

2.1. Physical–Chemical Analyses and Reagents

The reagents used in the assay were of analytical grade, except for metformin (MET), whose commercial formula comprised 500 mg capsules of metformin hydrochloride. The solutions were produced with distilled water. The microplastic consisted of polyethylene

microspheres (PMEs) purchased locally. The average diameter of the particles, according to the manufacturer, was 0.5 mm, and it was not necessary to perform any form of maceration or pulverizing of the material for characterization and performance of the sorption tests.

Metformin analysis was performed according to the spectrophotometric method with an absorbance at 232 nm, as proposed by Laporta et al. [20]. The equipment used was a Hach spectrophotometer, model DR 5000. The analytical curve was constructed with the commercial product in the range of 5 mg L^{-1} to 50 mg L^{-1} and $R^2 = 0.99$. All analyses were performed with samples previously filtered through quantitative filter paper.

2.2. Physicochemical Characterization of PMEs

The surface characteristics of the samples were studied via morphological characterization of the surface and elemental analysis (JEOL Scanning Electron Microscope, JSM—6610 and Thermo Scientific NSS Spectral Imaging with gold sputtering) to obtain images and analyze the adsorption and desorption of nitrogen (ASAP2020/Micromeristic). The specific surface areas of the PMEs, as well as the size and distribution of pores, were determined using ASAP (Accelerated Surface Area and Porosimetry) equipment. The BET model (Brunauer, Emmett and Teller) was applied to the nitrogen gas adsorption/desorption isotherms, which were obtained over a temperature range from 30 °C/303.15 K to −196 °C/77 K, at a heating rate of 10 °C min^{-1}, at 1 mmHg, with a relative pressure of 10^{-6} Pa.

Physicochemical characterization of the PMEs was performed by identifying the surface functional groups via Fourier transform spectroscopy in the infrared region (F-IRR) (Bruker Vertex 70 spectrometer), performing the test at the zero-charge point (pH_{PCZ}), according to the 11-point method presented by Essandoh et al. (2015), which consisted of adding 0.1 g of PMEs to 50 mL of 0.1 M KCl solution under different initial pH conditions ranging from 2 to 12. The suspensions were stirred at 125 rpm for 24 h at 25 °C. After the test period, the pH of each solution was measured, and a graph of the relationship between the initial pH and final pH was constructed to determine the pH at which the buffer effect occurred [21].

2.3. Adsorption–Desorption Assays in PMEs

The methodology for studying the adsorption–desorption dynamics of MET on polystyrene microplastics was designed to systematically evaluate the interaction mechanisms and influencing factors in this process. This section outlines the experimental approach used to quantify the adsorption capacity of polystyrene microplastics for metformin and to assess the subsequent desorption under controlled conditions, as shown in Figure 1. Adsorption experiments were conducted by exposing polystyrene microplastic particles to metformin solutions of varying concentrations, allowing for equilibrium studies that detail adsorption isotherms. Following adsorption, desorption studies were performed by transferring metformin-loaded microplastics to fresh aqueous media at pH 7 to investigate the release potential of metformin back into the environment. Analytical methods were utilized for precise quantification of metformin concentrations before and after the experiments. This methodology provides a comprehensive framework to elucidate the role of microplastic pollutants in the environmental transport and persistence of pharmaceutical contaminants.

Analyses of the effects of pH, PME dosage and temperature on adsorption were performed, as were assays to determine the adsorption capacity and rate of metformin, the latter using isotherms and adsorption kinetics, respectively. All the assays were performed in batches using an orbital shaker table (SoLab-223) maintained at a constant speed of 100 rpm and a temperature of 22 °C ± 1 °C in an acclimatized chamber. When necessary, the pH of each solution was adjusted with 0.1 M hydrochloric acid (HCl) or sodium hydroxide (NAOH).

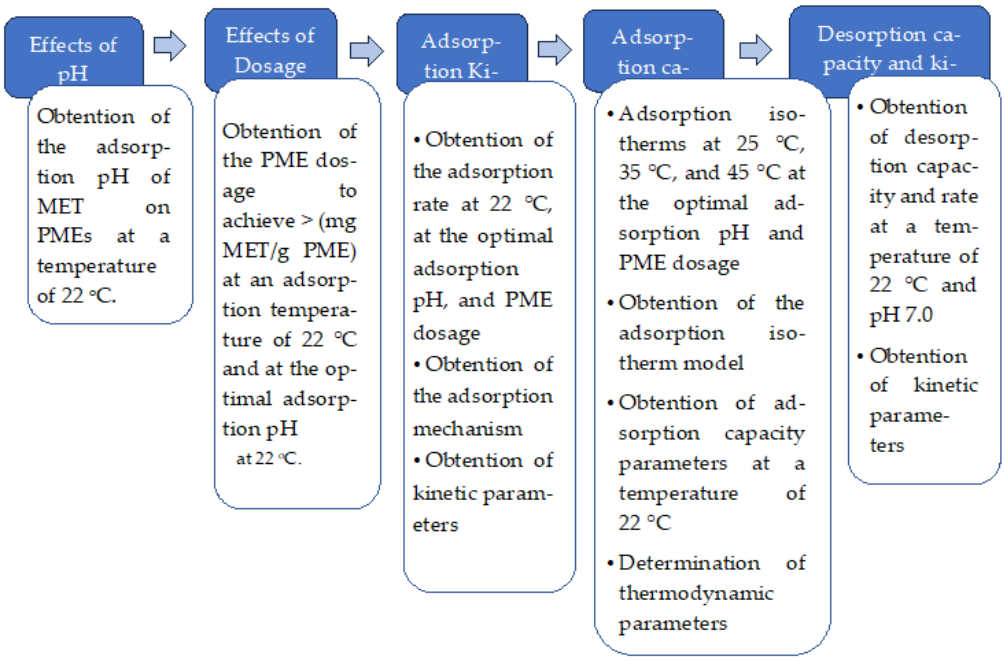

Figure 1. Flowchart of the experimental approach.

To evaluate the effect of pH on adsorption, 0.1 g of PMEs was added to 50 mL of metformin solution at a concentration of 20 mg L^{-1}, and the pH was adjusted to between 2 and 11 per unit [22]. To evaluate the influence of PME mass on metformin adsorption, masses of 0.05 g, 0.1 g, 0.15 g, 0.25 g, 0.5 g and 1.0 g of PMEs were added to 50 mL of metformin solution at a concentration of 20 mg L^{-1}. In both assays, the suspensions were kept under constant agitation (100 rpm) for a period of 24 h, and the results were expressed as the percentage of metformin removed (%) and the adsorption capacity—q_e (mg g^{-1}).

For the metformin adsorption capacity assay, 0.1 g of PMEs was added to 50 mL of metformin solution at concentrations of 10, 20, 40, 60, 100, 150 and 200 mg L^{-1}. The mixtures were kept under constant agitation for 24 h. At the end of the assay, the metformin concentration was determined, and the adsorption capacity values (q_e) were calculated (Equation (2)). The adsorption parameters were obtained via the Langmuir and Freundlich adsorption isotherm models [23].

The adsorption kinetics of metformin on PMEs were evaluated by maintaining 0.1 g of PMEs in 50 mL of metformin solution with a concentration of 20 mg L^{-1}, under constant agitation and temperature. At determined time intervals, aliquots of this mixture were collected to determine the amount of metformin remaining. The assay was terminated when the concentration of metformin in the solution remained constant [24]. To obtain the kinetic parameters, the metformin adsorption capacity data as a function of time (q_t) were fitted to pseudo-first-order models [25,26].

To evaluate the effect of temperature on the adsorption process, adsorption isotherm tests were performed at 25 °C, 35 °C and 45 °C. PMEs (0.05 g) were added to 50 mL of metformin solution at concentrations of 40, 60, 100, 150 and 200 mg L^{-1} [27]. The suspensions were kept under constant agitation for 24 h. The thermodynamic parameters obtained were the free energy change (ΔG°), enthalpy change (ΔH°), and entropy change (ΔS°).

Desorption capacity and kinetics assays were conducted in batches using an orbital shaker table (SoLab-223), maintained at a constant speed of 100 rpm, and a temperature of 22 °C ± 1 °C, in a climatized chamber. The regenerating solution was distilled water with 6.0 < pH < 7.0 [28].

PMEs saturated with metformin from the adsorption capacity tests were used. The amount of metformin desorbed was calculated from the concentration of metformin in

the fluid phase, either at time or at equilibrium, via Equation (1), whereas the amount of metformin retained in the PMEs after the desorption test was calculated via Equation (2).

$$q_d = C_r \times \frac{V}{m} \quad (1)$$

$$q_{rs} = q_e - q_d \quad (2)$$

where q_d is the amount of metformin desorbed from the PMEs (mg g^{-1}); q_{rs} is the amount of metformin retained in the PMEs after desorption (mg g^{-1}), q_e is the amount of adsorbed metformin (at equilibrium) obtained in the adsorption assay (mg g^{-1}), C_d is the concentration of metformin desorbed in the fluid phase at any time t or at equilibrium (mg L^{-1}); V is the volume of regenerating solution (L); and m is the mass of PMEs (g).

3. Results and Discussion

3.1. Physicochemical Characterization of PMEs

Visualization of the surface area of the PMEs by scanning electron microscopy (SEM) revealed that the microspheres do not have a defined standard shape (Figure 2a), which is characteristic of the amorphous shape of polyethylene [29]. It is still possible to verify that its surface has high roughness but low porosity, as evidenced in Figure 2b–d.

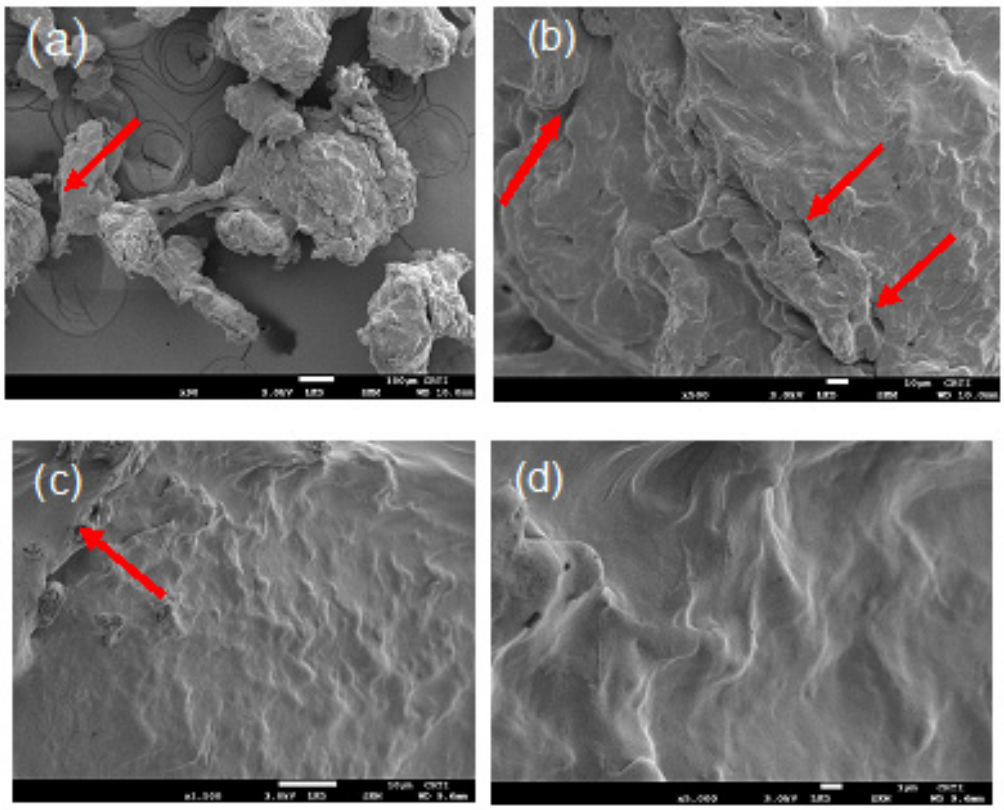

Figure 2. Scanning electron microscopy images of PMEs used in this study. Magnification: (**a**) 90×, (**b**) 500×, (**c**) 1500×, and (**d**) 5000×. Arrows indicate the presence of cracks on the surface of the PMEs.

Although it was not possible to verify the porosity of the samples, at the analyzed points, cracks could also contribute to increasing the surface area of the material and thus provide a greater number of active sites for adsorption, an attribute inherent to an adsorbent solid, indicating the possible ability of PMEs to retain compounds on their surface [30].

The analysis of the curves obtained from the N_2 adsorption and desorption isotherms (Figure 3) confirmed the surface structure observed via SEM. According to Thommes et al. [31], the curves obtained for the PMEs (Figure 3) are classified by the IUPAC as

class III, which describes the solid surface of nonporous or macroporous materials whose interactions between the adsorbent and adsorbate are relatively weak and without an identifiable monolayer.

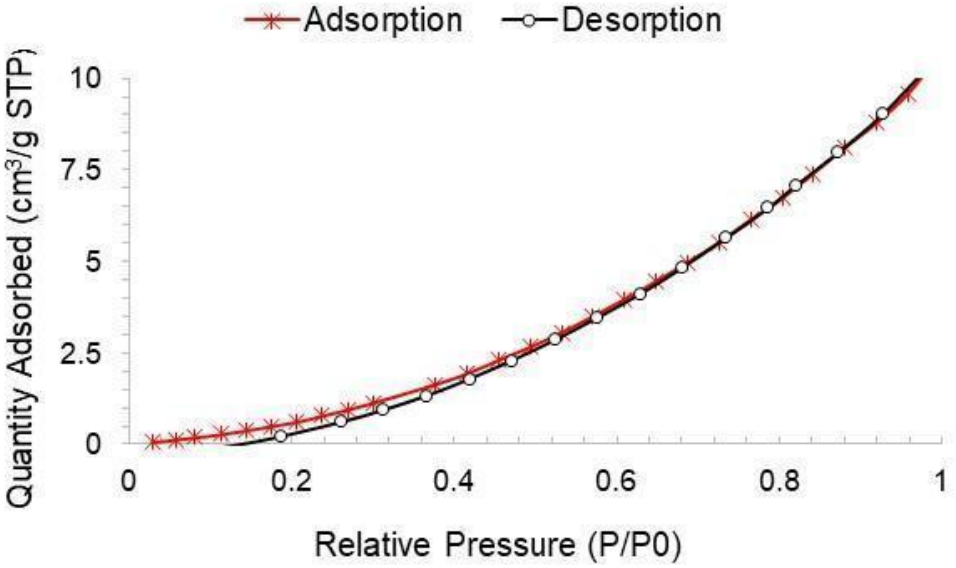

Figure 3. N_2 adsorption and desorption curves of the PMEs.

The surface area obtained for the PMEs was 17.56 m^2 g^{-1}, with a mean volume and pore size of 0.02 cm^3 g^{-1} and 37.26 Å, respectively. In the literature, these values are different; for example, [32] identified an area of 0.0062 m^2 g^{-1} for polyethylene extracted from a facial scrub. Wang et al. [8] worked with commercial polyethylene particles and obtained surface areas, volumes and average pore sizes of 0.23 m^2 g^{-1}, 0.003 cm^3 g^{-1} and 320,848 Å, respectively; thus, an adequate comparison is not possible. However, the average size of MET molecules, which was obtained by the Chemsketch program by considering the greatest distance between the H atoms of the molecule, was 7.76 Å, and thus, is not an impediment to adsorption within the pores.

3.2. Influence of the pH of the Medium and the Mass of PMEs on the Adsorption of MET

The pH of the medium is one of the parameters that most affects the adsorption of ionizable organic molecules, both because of its influence on the surface charge of the adsorbent material, which depends on its point of zero charge (ph_{ZCP}), and on the speciation of the organic contaminant.

According to Guan et al. [33], the surfaces of certain microplastics have relatively low ph_{ZCP} values between 4.0 and 7.0. For the PMEs under study, the ph_{ZCP} was 6.5; thus, in systems with pH values lower than 6.5, a positive charge is created on the MP surface due to protonation of its hydrated surface, whereas for pH values higher than 6.5, surface deprotonation occurs, thus leading to the formation of negative surface charges [34].

The metformin molecule (1,1-dimethylbiguanide HCl) is considered a cationic compound composed of two guanidine groups. The molecule has two pk values (2.8 and 11.5) and three structures as a function of pH (diprotonated at pH < 2.8, monoprotonated at 2.8 < pH < 11.5 and neutral at pH > 11.5), according to the schemes shown in Figure 4 [35].

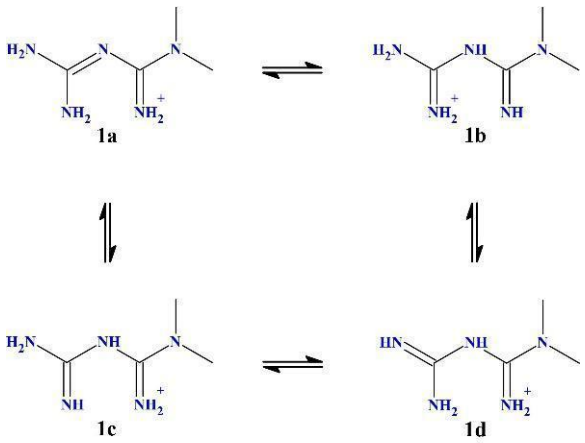

Scheme 1

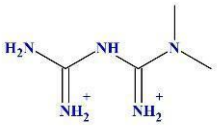

Scheme 2

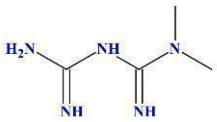

Scheme 3

Figure 4. Illustration of the structure of the metformin molecule as a function of the pH of the medium [35]. Scheme 1—monoprotonated, Scheme 2—diprotonated, and Scheme 3—neutral.

Figure 5 shows the MET adsorption capacity values for different pH values.

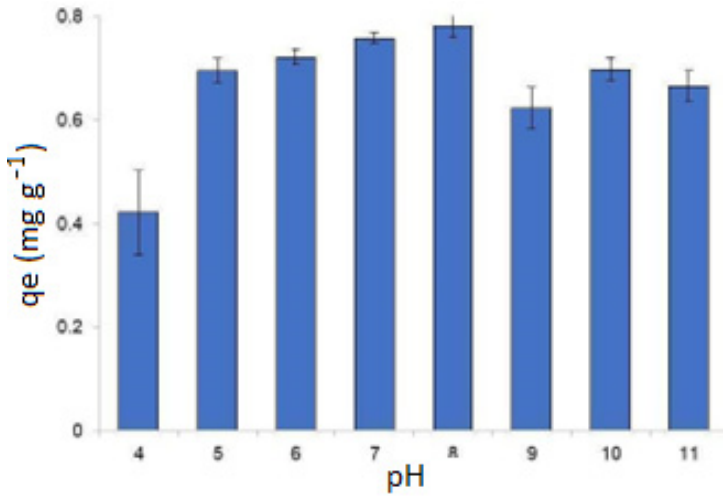

Figure 5. MET adsorption capacity as a function of pH.

For pH values lower than 4, it was not possible to obtain the adsorption capacity because it was not possible to visually perceive the MET precipitation. Desai et al. [36]

reported that at acidic pH values (1.2 and 4.5), the dissolution rates of metformin hydrochloride were lower than those observed at pH = 6.8. When protonated, the ability of metformin molecules to form hydrogen bonds increases, leading to better solvation in aqueous media [37] and consequently an increase in their hydrodynamic radius, resulting in lower diffusion coefficients during protonation [36].

At other pH values, no significant variations in the adsorption capacity of MET were observed. Between pH 5 and 11, the results remained in the range between 0.62 mg g^{-1} (pH = 9.0) and 0.78 mg g^{-1} (pH = 8.0). According to the pKa values of the MET molecule, in this pH range, there is a predominance of the monoprotonated structure of the molecule (Figure 4, Scheme 1). As the ph_{ZCP} of the PMEs obtained was 6.5, the MET was able to interact with both the positively and negatively charged surfaces. It is believed that this behavior is linked to the possible conformations of the electronic structure of the molecule resulting from the tautomeric forms of the guanidine groups. Bharatam, Patel and Iqbal [38], through studies of the electronic structure of biguanides, demonstrated the existence of 10 interconvertible tautomeric forms due to electron delocalization, either by delocalization of the lone pairs of electrons in the nitrogen of the amine group or by delocalization of π electrons. This phenomenon causes a concentration of electron density in the molecule, creating negative and positive potentials in the structure.

Regarding the influence of SEM mass on MET adsorption (Figure 6), a decrease in adsorption capacity was observed with increasing PME dosage. This behavior is similar to that observed for adsorbent materials produced from biomass [39] and occurs because of the greater availability of active sites for adsorption due to the increase in the mass of PMEs [40].

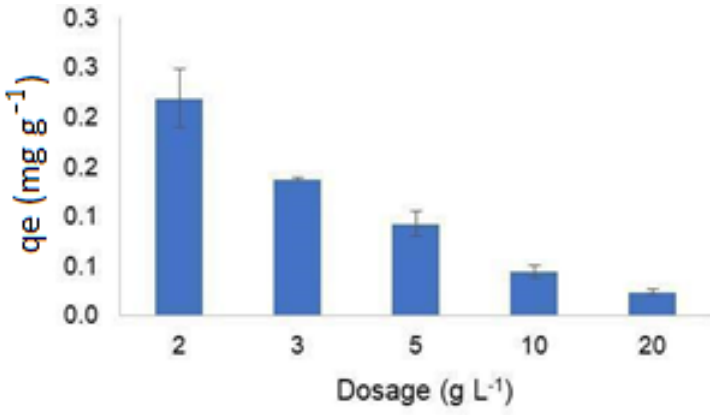

Figure 6. Adsorption capacity (q_e) of MET as a function of the mass of PMEs.

The adsorption capacity behavior shown in Figure 6 may have a worrying impact on the aquatic environment. According to a study by Divine et al. [41], the number of MP particles observed in surface water ranges from 600 to 1305 particle /m^3, in seawater from 30 to 1110 particles/m^3, and in sanitary sewage from 965 to 7800 particles/m^3. Thus, in media containing contaminants, such as metformin, the surface of the MP particles will have greater adsorption capacity because of the low proportion of MPs.

3.3. Study of the Adsorption Capacity

The adsorption data obtained in the assays fit only the Freundlich model (R^2 = 0.9428). Figure 7 shows the adsorption isotherms and fits of the data to the Freundlich model.

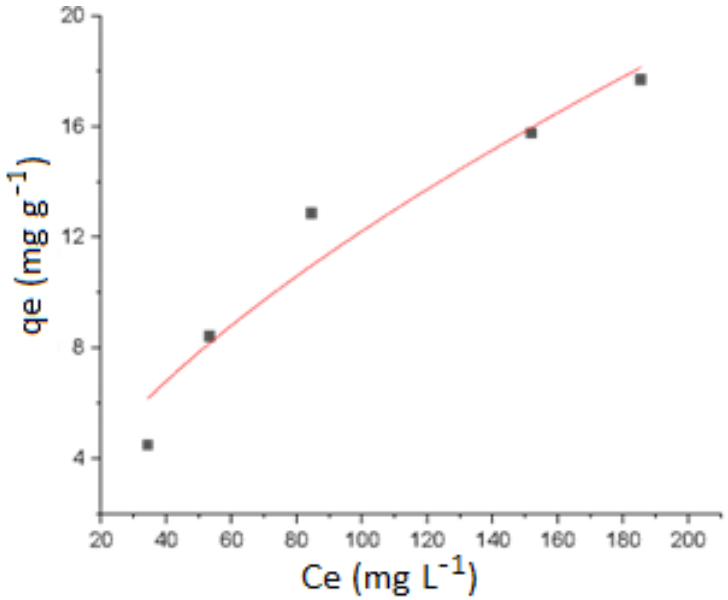

Figure 7. Adsorption isotherms and data fit to the Freundlich model.

In the literature, the interactions between organic compounds and microplastics are predominantly represented by this model. In this case, the adsorption of metformin onto PMEs under the test conditions occurred in multiple layers on an energetically heterogeneous surface, indicating that physical adsorption was predominant [42].

The parameters n_a and Ka_f of the Freundlich equation describe the nonlinearity of sorption and the affinity of the adsorbate on the adsorbent. In the present study, the value of $n_a < 1$ (0.64) suggests a decrease in the sorption affinity of MET with increasing initial concentration in the aqueous phase, whereas the value of Ka_f low (0.21 mg g^{-1}) reflects the low affinity of MET for MP beads.

Metformin is considered a hydrophilic compound because its log K_{ow} (−1.2) value is <2.0, so the predominant sorption interactions with the surface of the PMEs were not hydrophobic. Therefore, the partition coefficient between the liquid phase and the solid phase (microplastic) (K_D), calculated from Henry's region (linear portion) of the isotherms, was 151.0 L g^{-1} (R^2 = 0.99), and the Log K_{ow} value was −1.21, values that were significantly lower than those obtained for hydrophobic organic compounds by other authors (Table 1).

Table 1. Valores de KD para adsorção de diferentes compostos.

Composto	Temp. (°C)	K_D (Lg^{-1})	LogK_{ow}	Classification	Ref.
Metformin	25	151.0	−1.21	HFI	This research
Propranolol	24	2.3	3.48	HFO	[30]
Sertraline		3.33	5.29	HFO	
Phenanthrene	25	12.8×10^6	4.46	HFO	[43]
Nitrobenzene		97.7×10^6	1.85	HFO	
Naphthalene		67.6×10^6	3.3	HFO	
Carbendazim	25	1.28×10^{-3}	-	HFO	[42]
Difenoconazole		0.63×10^3	-	HFO	
Malathion		0.08×10^3	-	HFO	
Diflubenzuron		0.26×10^3	-	HFO	

Note: HFI—hydrophilic; HFO—hydrophobic.

As the assay was performed at pH = 8.0, the surfaces of the PMEs are predominantly negative (pH_{PCZ} = 6.5), whereas MET is present in its monoprotonated form (Figure 4, Scheme 1), which suggests that electrostatic interactions have occurred [44].

Razanajatovo et al. [30] also proposed the same assumption when studying the adsorption of the drugs propranolol and sertraline, both hydrophilic compounds, on PE particles at pH values above the zero charge point and above the pKa of microplastics and drugs, respectively.

Furthermore, in the production processes of polymers, different additives are used to improve their plastic properties, which may confer diverse functional groups on their surfaces [43]. For this reason, Zhao et al. [45] emphasized that interactions such as hydrogen bonds, π-π interactions and van der Waals forces should not be ignored in adsorption processes involving MPs.

In the case of PE, the addition of oleamide and erucamide is common for improving the characteristics of plastic films [46]. These additives have polar oxygenated functional groups that, when exposed to the PE surface, can form hydrogen bonds with compounds that have secondary amines in their structure [42], as is the case with MET.

The presence of functional groups in the PMEs and their possible interactions with MET were analyzed via the FT-IR method, and the spectra before and after the adsorption of MET are shown in Figure 8.

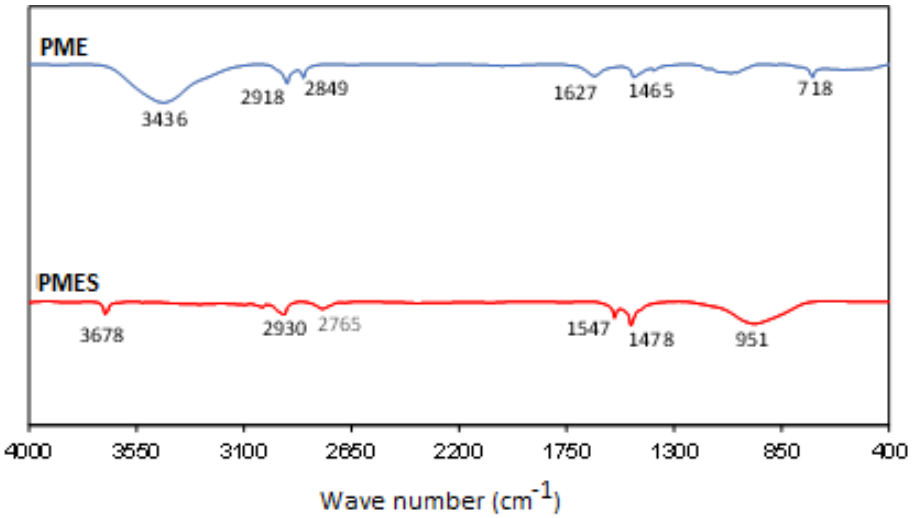

Figure 8. FTIR spectra of the PMEs before adsorption (PME) and after adsorption of metformin (PMES).

In the PME spectrum shown in Figure 8, peaks were identified at 2918 cm^{-1} and 1465 cm^{-1}, corresponding to the symmetric stretching and deformation of $–CH_2$, respectively, and at 718 cm^{-1}, they were attributed to wobble deformation [47]. These peaks, together with those observed at 2848 cm^{-1} and 2918 cm^{-1} ($–CH_2$ group), suggest that the material of the microspheres corresponds to PE (Lan et al., 2021) [42]. The peak at 3436 cm^{-1} corresponds to the –OH group [48].

After MET adsorption (PMES spectrum), peaks were identified for the metformin molecule at 3678 cm^{-1} and 1478 cm^{-1}, attributed to the stretching of the N–H and C–N bonds, respectively, and a peak corresponding to bending =CH was identified at 951 cm^{-1}. Furthermore, the disappearance of the band at 3436 cm^{-1} suggests the presence of hydrogen bonds between –OH groups in the PME and the secondary amine in the MET image. In addition to the disappearance of bands, other aspects that suggest interactions between the functional groups of PMEs and MET include reductions or shifts in peaks after adsorption [49].

3.4. Adsorption Kinetics

Figure 9 shows the results of MET removal as a function of time.

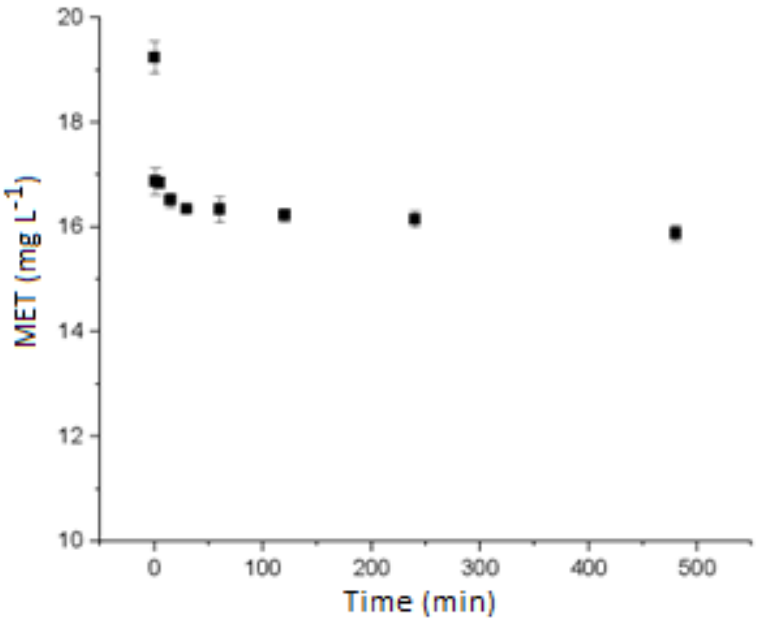

Figure 9. MET removal as a function of time.

The reaction occurred quickly during the first 15 min of the test and tended to reach the equilibrium state during the first 60 min of the test. The decrease and subsequent equilibrium in the adsorption rate with time is due to the occupation of active sites on the surface of the PMEs followed by their full occupation [15] or by the decrease in the concentration of MET in the medium, generating a reduction in the driving force [34]. The mean concentration remaining at equilibrium was 16.8 mg L^{-1}, corresponding to an average removal capacity of 1.54 ± 0.0071 mg g^{-1} and a removal efficiency of 19.85%. Lin et al. [50] studied the adsorption of Basic Blue 9 and Reactive Red 120 onto particles of polyethylene, polyethylene terephthalate, polystyrene, high-density polyethylene and low-density polyethylene and reported similar behavior, i.e., rapid initial adsorption followed by lower velocities until equilibrium; however, the time periods for the adsorption of the dyes were on the order of days, with adsorption capacities at equilibrium ranging from 15.90 mg g^{-1} to −18.80 mg g^{-1} for Reactive Red 120, and between 15.55 mg g^{-1} and 18.54 mg g^{-1} for Basic Blue 9. Atugoda et al. [15] studied the adsorption of the antibiotic ciprofloxacin onto polyethylene particles and the adsorption equilibrium in a 3 h assay, and reported a capacity of 2.1 mg g^{-1}. When studying the adsorption of triclosan onto PE particles, Chen et al. [51] obtained results closer to those of the present study, with an eq and equilibrium time of 30 min and 1.21 mg g^{-1}, respectively.

The transfer of a contaminant from the liquid phase to the surface of a solid occurs via different mechanisms, such as surface adsorption (external diffusion), internal diffusion and mechanisms of interaction between the adsorbate and adsorbent [52]. Kinetic models are commonly used to obtain information about the mechanisms that govern adsorption, the most common of which are the pseudo-first- and pseudo-second-order models.

Figure 10 shows the fit of the results to the pseudo-first- and pseudo-second-order kinetic models, while Table 2 shows the values of the parameters obtained for each model.

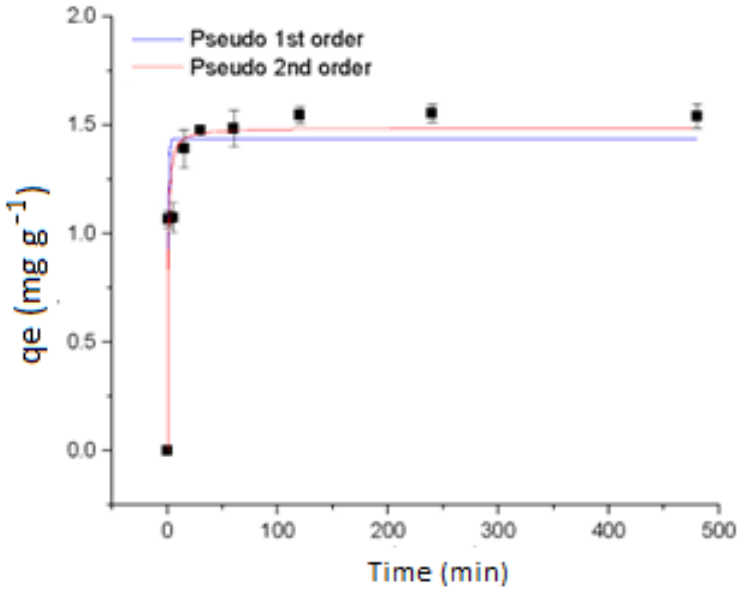

Figure 10. Adsorption kinetics and data fit to the pseudo-first- and pseudo-second-order models.

Table 2. Kinetic parameters for MET adsorption onto PMEs.

		Pseudo-First Order	**Pseudo-Second Order**
Parameter	Unit	$q_t = q_e\left(1 - e^{-k_1 t}\right)$	$q_t = \frac{k_2 q_e^2 t}{1+k_2 q_e t}$
$q_{e(exp.)}$	mg g^{-1}	1.5473	1.5473
$q_{e(calc.)}$	mg g^{-1}	1.4392	1.4879
K_1	min^{-1}	1.3240	-
K_2	g $mg^{-1}min^{-1}$	-	1.2166
R^2	-	0.9139	0.9519

Note: Assay performed with an initial concentration of MET = 20 mg L^{-1}, pH = 8.0, and temperature = 22 °C ± 1 °C. Parameters: k_1—pseudo-first-order rate constant; k_2—pseudo-second-order rate constant; q_e—amount of MET adsorbed at equilibrium; q_t—amount of MET adsorbed at a given time; t—time (min).

With respect to the kinetic parameters (Table 2), the highest value of R^2 and $q_{e(calc)}$ closest to $q_{e(exp)}$ was for the pseudo-second-order model, indicating that the adsorption under study could be represented by a process in which chemical interactions between the adsorbent and adsorbate are predominant (chemosorption) [53] and controlled by limitations of active sites on the surface of PMEs for MET interaction [51].

In the literature, the pseudo-second-order model has been widely used to describe the mechanism of interaction between PM particles and organic contaminants. However, in the present study, as in the one developed by Lu et al. [54], the fit to the pseudo-first-order model also presented satisfactory parameters (R^2 = 0.91, $eq_{e(exp.)}$ = 1.44), which implies that physical phenomena dominate the adsorption process. Thus, as both models obtained satisfactory fits, it is suggested that both physical and chemical mechanisms contribute to the adsorption of MET onto the PMEs under the study conditions.

To evaluate the MET adsorption rate after the initial adsorption stage, the Webber–Morris intraparticle diffusion method was used, plotting q_t as a function of $t^{0.5}$ [55], and the results are shown in Figure 11.

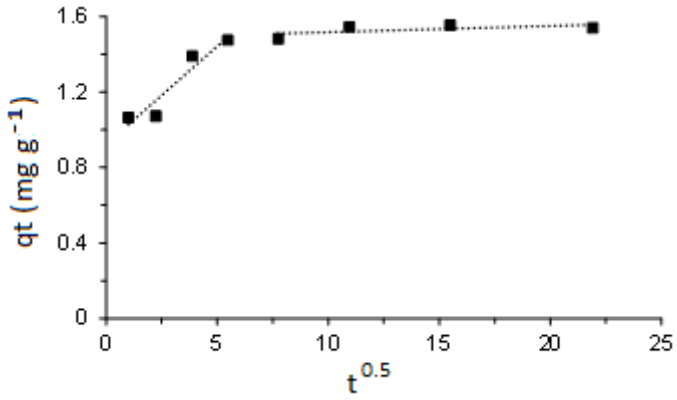

Figure 11. Fitting data of MET adsorption onto PME spheres. Note: The assay was performed with an initial concentration of MET = 20 mg L^{-1}, pH = 8.0, and temperature = 22 °C ± 1 °C.

The presence of two stages (Figure 11) means that the adsorption of MET onto PMEs is a heterogeneous process controlled by two adsorption mechanisms [55]. In the first stage, a greater slope of the line is observed; therefore, a higher rate of MET occupancy occurs at the external activated sites, followed by diffusion in the internal pores [51]. In the second stage, represented by the plateau, there is an important external mass transfer equilibrium between the MET in the liquid phase and the MET adsorbed onto the PMEs, suggesting a dynamic adsorption/desorption equilibrium [53].

Furthermore, as none of the lines pass through the origin, it can be inferred that both liquid film diffusion and intraparticle diffusion simultaneously control the MET adsorption process [51].

3.5. Influence of Temperature on MET Adsorption in PMEs

The influence of temperature on the adsorption of MET onto PMEs was analyzed via adsorption isotherms at temperatures of 25 °C, 35 °C and 45 °C, as shown in Figure 12, and the thermodynamic parameters obtained from the Gibbs free energy and van't Hof equations are shown in Table 3.

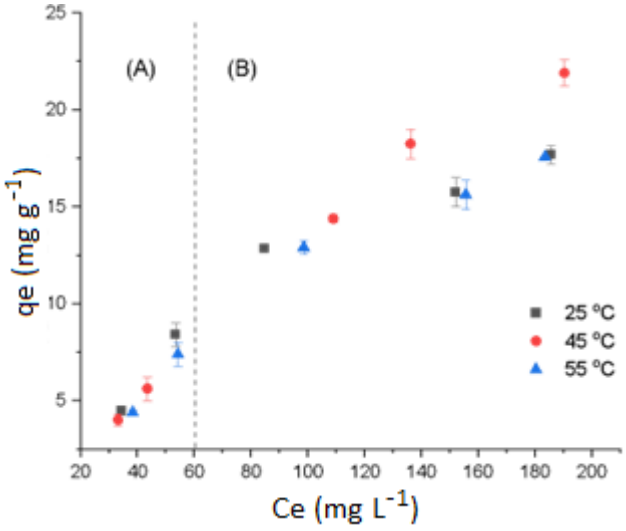

Figure 12. Influence of temperature on MET adsorption onto PMEs.

Table 3. Thermodynamic parameters for the adsorption of MET onto PMEs.

Temperature (°C)	K_d	ΔG_{ads}	ΔH_{ads}	ΔS_{ads}
	$K_d = \frac{q_e}{C_e}$	$\Delta G = -RTlnK_d$	$\ln(K_d) = \frac{\Delta S}{R} - \frac{\Delta H}{R.T}$	
25	0.15	46.33		
45	0.13	52.19	40.99	−0.29
55	0.13	55.12		

Note: ΔG—change in Gibbs free energy T—temperature (K), R—universal gas constant 8.314 (JK^{-1} mol^{-1}), K_d—equilibrium constant, ΔS—entropy (J mol^{-1} K^{-1}) and ΔH—enthalpy (J mol^{-1}).

Figure 12 shows that the adsorption of MET onto PMEs with respect to temperature exhibited two distinct behaviors. For initial MET concentrations of 40 mg L^{-1} and 60 mg L^{-1} (region A), there was no influence of temperature on the adsorption capacity, whereas for initial concentrations of 100 mg L^{-1}, 150 mg L^{-1} and 200 mg L^{-1} (region B), the temperature variation was more relevant in the process, but in a limited way. As shown in Figure 12, the increase in temperature from 25 °C to 45 °C increased the capacity of adsorption of the MET onto the PMEs; however, when the tests were performed at 55 °C, the adsorption decreased.

Chen et al. [56] reported the same behavior when studying the adsorption of tri-n-butyl phosphate and tris(2-chloroethyl) phosphate onto polyethylene microparticles and reported that the decrease in the adsorption capacity of contaminants with increasing temperature occurred as a result of decreased van der Waals interactions or disruption of hydrogen bonds between the adsorbate and microplastic due to increased random motion of molecules.

Regarding the thermodynamic adsorption parameters ΔG_{ads}, ΔH_{ads} and ΔS_{ads} (Table 3), positive values of ΔH_{ads} (40.99 J mol^{-1}) and ΔG_{ads} (46.33 J mol^{-1}) indicate that the adsorption is endothermic and nonspontaneous, respectively. These results indicate that the process of MET adsorption onto PMEs requires the input of additional external energy in the range of 25–45 °C [57]. This result indicates that, although they are not predominant, hydrophobic interactions between MET and PMEs also occur because as the temperature increases, hydrophobic interactions are potentiated [53]. Evaluating changes in ΔS_{ads} is a way to measure the repulsive or binding force in a system, which is related to the spatial arrangement of the adsorbent interface. In this case, the result of $\Delta S_{ads} < 0$ suggests a lower randomness at the solid/solution interface during the adsorption process, which indicates a weak affinity between MET and PMEs [58].

3.6. Desorption Capacity of MET of the Surface of PMEs

The MET desorption behavior of PMEs after 24 h is presented in Figure 13. The desorption capacity (qd) represents the amount of MET present in the regenerating solution after a 24 h contact period, with PMEs saturated with varying amounts of MET (qa), as determined from the adsorption isotherm experiment conducted at 45 °C.

The desorption equilibrium results presented in Figure 13 indicate that the desorption capacity increases as a function of the initial amount of adsorbed MET (qa). However, when the percentage of desorption is analyzed, it initially decreases with increasing amounts of MET adsorbed onto the PMEs, from 26.14% to 9.84%, and then remains at this value regardless of the amount of MET adsorbed onto the PMEs.

Desorption was likely favored by the pH and temperature of the liquid medium used. As the adsorption of MET onto the PMEs proved to be an endothermic process, low temperatures favored the desorption process. In addition, the pH value of the desorption assay, which is close to neutral, may also influence desorption because, under these conditions, the surface of the PMEs has a lower tendency to present a negative surface (pH_{PCZ} = 6.5), whereas the MET molecules can have a diprotonated structure (Figure 4, Scheme 2), which would lead to repulsion between the MET and microplastic. Mcdougall et al. [59] reported

that the desorption of cationic pharmaceuticals was increased at low pH values and, similar to the present study, concluded that electrostatic repulsion favored this process.

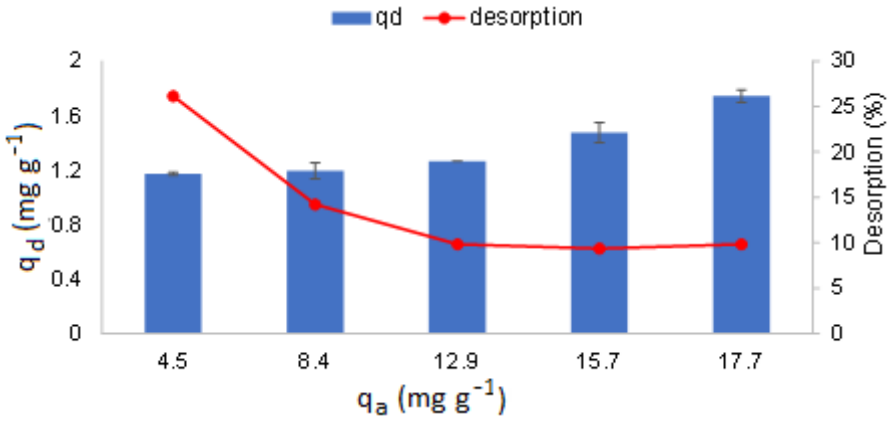

Figure 13. Desorption capacity (q_d) and efficiency (%) of the MET of the PMEs. Note: Assay conditions: 50 mL of regenerating solution (deionized water) with 6.0 < pH < 7.0. Temperature—22 °C.

As for the adsorption isotherms, the desorption data fit best and fit only the Freundlich model (R^2 = 0.72). Table 4 shows the values of the desorption parameters obtained after fitting the results to the Freundlich model and the hysteresis index (HI) values [60] obtained for five MET concentrations at equilibrium (C_e) at 25 °C.

Table 4. Values of the adsorption and desorption parameters adjusted to the Freundlich model and the hysteresis index (HI) obtained for the adsorption and desorption assay.

C_e (mg L^{-1})	n_a	n_d	$k^a{}_f$ (mg g^{-1})	$k^d{}_f$ (mg g^{-1})	HI
					$HI = \frac{q_e^d - q_e^a}{q_e^a}$
34.37					<0
53.43					<0
84.62	0.64	2.22	0.21	1.10	<0
141.99					<0
195.46					<0

Note: qe^a and qe^d are the amounts of MET adsorbed at equilibrium in the PMEs obtained in the single-cycle adsorption and desorption experiments, respectively. EC and equilibrium concentrations of MET in the aqueous phase.

A value of n_d > 1 (2.24) indicates that desorption is nonlinear and favorable, i.e., desorption can increase with increasing amounts of MET initially adsorbed onto PMEs, a phenomenon also observed by Wu et al. [60].

In the case where all HI values were <0, the adsorption of MET onto the PMEs was completely reversible, and no hysteresis occurred.

3.7. Desorption Kinetics

The desorption capacity and percentage desorption results, as shown in Figure 14A and 14B, respectively, demonstrate that MET desorption was quite fast. In the first minute of the test, there was a desorption (q_{td}) of 1.40 mg g^{-1} (88.6%) of desorbed MET, and equilibrium after 60 min with q_{ed} = 1.45 mg g^{-1} ± 0.008 mg g^{-1} (92.3%). These desorption percentage values for MET were significantly higher than those observed for adsorption (19.85%). This result reflects the hydrophilic characteristics of the MET molecule.

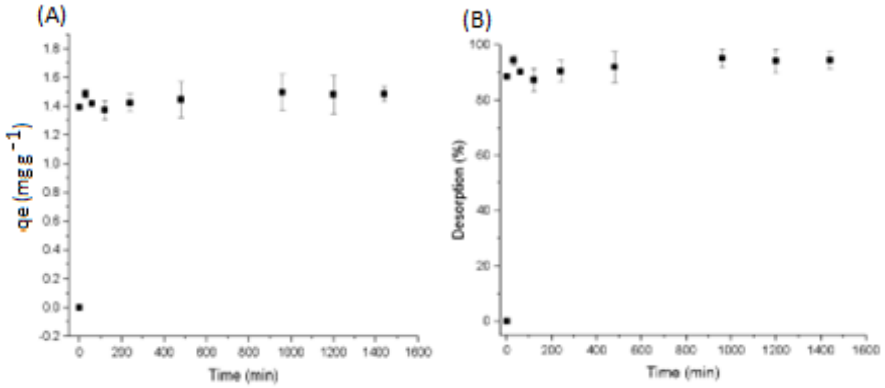

Figure 14. Desorption kinetics. (**A**) Desorption capacity q_{td} (mg g^{-1}), and (**B**) % MET desorption. Note: 50 mL of deionized water, pH = 7.0, T = 22 °C, agitation = 100 rpm.

Other studies involving the adsorption of organic compounds onto polyethylene microplastics have also reported high desorption rates. Ju et al. (2023) reported 40% desorption of chlorpyrifos (organophosphate insecticide).

The fit of the data to the kinetics models was satisfactory for both models ($R^2 > 0.99$). The pseudo-first-order and pseudo-second-order desorption constants were 3.20 min^{-1} and 16.08 g mg^{-1} min^{-1}, respectively. A comparison of the values of these desorption constants with the respective adsorption constants (k_1 = 1.32 min^{-1} and k_2 = 1.22 g mg^{-1} min^{-1}) indicates that the desorption rate was significantly greater.

Both the reversibility and the high desorption rates of MET on PMEs demonstrate that polyethylene can release metformin into aquatic environments under the pH and temperature conditions commonly observed in many water bodies, which may pose a potential environmental risk.

3.8. Environmental Considerations

Previous studies have demonstrated both the frequent presence of polyethylene microplastics in aquatic environments and their ability to transport hydrophobic contaminants. However, the present study revealed that polyethylene particles can also transport compounds that are considered hydrophilic, such as metformin (MET).

MET adsorption can occur at pH values > 5.0, which comprises both industrial effluents and domestic sewage. It was clear that the adsorption was fast and that low PME/MET ratios considerably increased the adsorption capacity of the particles.

The desorption process in waters with pH values close to 7.0 was relatively fast and reached high percentages. This finding demonstrates that MET bound to polyethylene particles, when in contact with environmental water, becomes bioavailable [59], indicating that PMEs can be considered MET vectors.

4. Conclusions

The present study focused on the adsorption of MET, a hydrophilic compound, onto polyethylene microbeads (PMEs).

The results showed that pH values above 5.0 had little influence on MET adsorption onto PMEs. However, lower ratios of microplastics relative to MET concentrations in the liquid phase could enhance MET adsorption capacity.

Adsorption occurred rapidly within the first 15 min, reaching equilibrium at 60 min, with a media removal capacity of 1.54 mg g^{-1} ± 0.00713 mg g^{-1} and removal efficiency of 19.85%. Desorption was faster, with 1.3929 mg g^{-1} (88.6%) of MET desorbed, and equilibrium reached at 60 min, with qed = 1.4472 mg g^{-1} ± 0.008 mg g^{-1} (92.3%).

The adsorption isotherm data fitted only the Freundlich model (R^2 = 0.9428), with parameters indicating decreasing sorption affinity (n < 1; 0.63945) as MET concentration increased, while a low Kaf (0.21156 mg g^{-1}) reflected MET's low affinity for the PMEs.

In desorption isotherms, nd > 1 indicated nonlinear and favorable desorption, meaning it could increase with higher initial MET adsorption. Hysteresis index (HI) values of <0 suggested that MET adsorption onto PMEs was fully reversible, with no hysteresis occurring.

These findings emphasize the potential for polyethylene to release metformin into aquatic environments under typical pH and temperature conditions, posing an environmental risk.

Author Contributions: Conceptualization, L.G.G., R.M.F.C. and F.J.C.T.; methodology, L.G.G. and R.M.F.C.; validation, R.M.F.C. and F.J.C.T.; formal analysis, R.M.F.C.; investigation, L.G.G. and R.M.F.C.; resources, R.M.F.C. and F.J.C.T.; data curation, R.M.F.C.; writing—original draft preparation, L.G.G. and R.M.F.C.; writing—review and editing, L.G.G., R.M.F.C. and F.J.C.T.; supervision, R.M.F.C.; project administration, R.M.F.C.; funding acquisition, R.M.F.C. All authors have read and agreed to the published version of the manuscript.

Funding: This research received no external funding.

Data Availability Statement: The research data is unavailable due to privacy.

Acknowledgments: The authors acknowledge the Coordenação de Aperfeiçoamento de Pessoal de Nível Superior CAPES Foundation, Brazil, for a scholarship.

Conflicts of Interest: The authors declare no conflicts of interest.

References

1. Amaral-Zettler, L.A.; Zettler, E.R.; Mincer, T.J. Ecology of the plastisphere. *Nat. Rev. Microbiol.* **2020**, *18*, 139–151. [CrossRef] [PubMed]
2. Chia, W.Y.; Tang, D.Y.Y.; Khoo, K.S.; Lup, A.N.K.; Chew, K.W. Nature's fight against plastic pollution: Algae for plastic biodegradation and bioplastics production. *Environ. Sci. Ecotechnol.* **2020**, *4*, 100065. [CrossRef] [PubMed]
3. Rodrigues, S.; Almeida, C.M.R.; Silva, D.; Cunha, J.; Antunes, C.; Freitas, V.; Ramos, S. Microplastic contamination in an urban estuary: Abundance and distribution of microplastics and fish larvae in the Douro estuary. *Sci. Total. Environ.* **2019**, *659*, 1071–1081. [CrossRef] [PubMed]
4. Rochman, C.M.; Hoh, E.; Hentschel, B.T.; Kaye, S. Long-Term Field Measurement of Sorption of Organic Contaminants to Five Types of Plastic Pellets: Implications for Plastic Marine Debris. *Environ. Sci. Technol.* **2013**, *47*, 1646–1654. [CrossRef]
5. USEPAO. Microplastics Research. 2022. Available online: https://www.epa.gov/water-research/microplastics-research (accessed on 14 November 2024).
6. Hu, Y.; Zhou, L.; Zhu, J.; Gao, J. Efficient removal of polyamide particles from wastewater by electrocoagulation. *J. Water Process. Eng.* **2023**, *51*, 103417. [CrossRef]
7. Ziembowicz, S.; Kida, M. The effect of water ozonation in the presence of microplastics on water quality and microplastics degradation. *Sci. Total. Environ.* **2024**, *929*, 172595. [CrossRef]
8. Wang, F.; Gao, J.; Zhai, W.; Liu, D.; Zhou, Z.; Wang, P. The influence of polyethylene microplastics on pesticide residue and degradation in the aquatic environment. *J. Hazard. Mater.* **2020**, *394*, 122517. [CrossRef]
9. Wagstaff, A.; Petrie, B. Enhanced desorption of fluoxetine from polyethylene terephthalate microplastics in gastric fluid and sea water. *Environ. Chem. Lett.* **2022**, *20*, 975–982. [CrossRef]
10. Lares, M.; Ncibi, M.C.; Sillanpää, M.; Sillanpää, M. Occurrence, identification and removal of microplastic particles and fibers in conventional activated sludge process and advanced MBR technology. *Water Res.* **2018**, *133*, 236–246. [CrossRef]
11. Keller, A.S.; Jimenez-Martinez, J.; Mitrano, D.M. Transport of Nano- and Microplastic through Unsaturated Porous Media from Sewage Sludge Application. *Environ. Sci. Technol.* **2020**, *54*, 911–920. [CrossRef]
12. Qi, R.; Jones, D.L.; Li, Z.; Liu, Q.; Yan, C. Behavior of microplastics and plastic film residues in the soil environment: A critical review. *Sci. Total. Environ.* **2020**, *703*, 134722. [CrossRef] [PubMed]
13. Liu, X.; Xu, J.; Zhao, Y.; Shi, H.; Huang, C.-H. Hydrophobic sorption behaviors of 17β-Estradiol on environmental microplastics. *Chemosphere* **2019**, *226*, 726–735. [CrossRef] [PubMed]
14. Miranda, M.N.; Ribeiro, A.R.L.; Silva, A.M.; Pereira, M.F.R. Can aged microplastics be transport vectors for organic micropollutants?—Sorption and phytotoxicity tests. *Sci. Total. Environ.* **2022**, *850*, 158073. [CrossRef] [PubMed]
15. Atugoda, T.; Wijesekara, H.; Werellagama, D.; Jinadasa, K.; Bolan, N.S.; Vithanage, M. Adsorptive interaction of antibiotic ciprofloxacin on polyethylene microplastics: Implications for vector transport in water. *Environ. Technol. Innov.* **2020**, *19*, 100971. [CrossRef]
16. Oliveira, Y.M.; Vernin, N.S.; Zhang, Y.; Maginn, E.; Tavares, F.W. Interaction Between Endocrine Disruptors and Polyethylene Nanoplastic by Molecular Dynamics Simulations. *J. Phys. Chem. B* **2024**, *128*, 2045–2052. [CrossRef]

17. Elizalde-Velázquez, G.A.; Gómez-Oliván, L.M.; García-Medina, S.; Hernández-Díaz, M.; Islas-Flores, H.; Galar-Martínez, M.; García-Medina, A.L.; Chanona-Pérez, J.J.; Hernández-Varela, J.D. Polystyrene microplastics mitigate the embryotoxic damage of metformin and guanylurea in Danio rerio. *Sci. Total. Environ.* **2022**, *852*, 158503. [CrossRef]
18. Occurrence of the Antidiabetic Drug Metformin and Its Ultimate Transformation Product Guanylurea in Several Compartments of the Aquatic Cycle—PubMed. Available online: https://pubmed.ncbi.nlm.nih.gov/24954924/ (accessed on 27 September 2024).
19. Souza, E.; Bittencourt, T.; Ferreira, R.; Oliveira, E.; Silva, N.; Silva, S.; Cadena, M.; Cadena, P. Exposição crônica ao cloridrato de metformina e à glibenclamida causa alterações comportamentais, glicêmicas e de mortalidade em Hemigrammus caudovittatus e Danio rerio. *Arq. Bras. De Med. Veter E Zootec.* **2019**, *71*, 1582–1590. [CrossRef]
20. Laporta, L.V.; de Brum, T.F.; Júnior FR, P.; Santos, M.R.; Gonçalves, C.A. Validação de método analítico para avaliação da qualidade de cápsulas de cloridrato de metformina manipuladas. *Rev. De Ciências Farm. Básica E Apl.* **2013**, *34*.
21. Park, J.; Regalbuto, J.R. A Simple, Accurate Determination of Oxide PZC and the Strong Buffering Effect of Oxide Surfaces at Incipient Wetness. *J. Colloid Interface Sci.* **1995**, *175*, 239–252. [CrossRef]
22. Herath, I.; Kumarathilaka, P.; Al-Wabel, M.I.; Abduljabbar, A.; Ahmad, M.; Usman, A.R.; Vithanage, M. Mechanistic modeling of glyphosate interaction with rice husk derived engineered biochar. *Microporous Mesoporous Mater.* **2016**, *225*, 280–288. [CrossRef]
23. Zhang, K.; Hamidian, A.H.; Tubić, A.; Zhang, Y.; Fang, J.K.; Wu, C.; Lam, P.K. Understanding plastic degradation and microplastic formation in the environment: A review. *Environ. Pollut.* **2021**, *274*, 116554. [CrossRef] [PubMed]
24. Dong, Q.; Yang, D.; Luo, L.; He, Q.; Cai, F.; Cheng, S.; Chen, Y. Engineering porous biochar for capacitive fluorine removal. *Sep. Purif. Technol.* **2021**, *257*, 117932. [CrossRef]
25. Choi, M.-Y.; Lee, C.-G.; Park, S.-J. Enhanced Fluoride Adsorption on Aluminum-Impregnated Kenaf Biochar: Adsorption Characteristics and Mechanism. *Water Air Soil Pollut.* **2022**, *233*, 435. [CrossRef]
26. Daifullah, A.; Yakout, S.; Elreefy, S. Adsorption of fluoride in aqueous solutions using KMnO4-modified activated carbon derived from steam pyrolysis of rice straw. *J. Hazard. Mater.* **2007**, *147*, 633–643. [CrossRef]
27. de Freitas, D.C. Adsorção e Dessorção do Corante Preto Reativo 5 em Solução Aquosa Utilizando Adsorvente Alternativo de lodo de Esgoto Sanitário (Biocarvão). 2020. Available online: http://repositorio.utfpr.edu.br/jspui/handle/1/5111 (accessed on 27 September 2024).
28. Chintala, R.; Mollinedo, J.; Schumacher, T.E.; Papiernik, S.K.; Malo, D.D.; Clay, D.E.; Kumar, S.; Gulbrandson, D.W. Nitrate sorption and desorption in biochars from fast pyrolysis. *Microporous Mesoporous Mater.* **2013**, *179*, 250–257. [CrossRef]
29. Lazrak, C.; Kabouchi, B.; Hammi, M.; Famiri, A.; Ziani, M. Structural study of maritime pine wood and recycled high-density polyethylene (HDPEr) plastic composite using Infrared-ATR spectroscopy, X-ray diffraction, SEM and contact angle measurements. *Case Stud. Constr. Mater.* **2019**, *10*, e00227. [CrossRef]
30. Razanajatovo, R.M.; Ding, J.; Zhang, S.; Jiang, H.; Zou, H. Sorption and desorption of selected pharmaceuticals by polyethylene microplastics. *Mar. Pollut. Bull.* **2018**, *136*, 516–523. [CrossRef]
31. Thommes, M.; Kaneko, K.; Neimark, A.V.; Olivier, J.P.; Rodriguez-Reinoso, F.; Rouquerol, J.; Sing, K.S.W. Physisorption of gases, with special reference to the evaluation of surface area and pore size distribution (IUPAC Technical Report). *Pure Appl. Chem.* **2015**, *87*, 1051–1069. [CrossRef]
32. Rozman, U.; Turk, T.; Skalar, T.; Zupančič, M.; Korošin, N.Č.; Marinšek, M.; Olivero-Verbel, J.; Kalčíková, G. An extensive characterization of various environmentally relevant microplastics—Material properties, leaching and ecotoxicity testing. *Sci. Total Environ.* **2021**, *773*, 145576. [CrossRef]
33. Guan, J.; Qi, K.; Wang, J.; Wang, W.; Wang, Z.; Lu, N.; Qu, J. Microplastics as an emerging anthropogenic vector of trace metals in freshwater: Significance of biofilms and comparison with natural substrates. *Water Res.* **2020**, *184*, 116205. [CrossRef]
34. Huang, X.; Liu, Y.; Liu, S.; Li, Z.; Tan, X.; Ding, Y.; Zeng, G.; Xu, Y.; Zeng, W.; Zheng, B. Removal of metformin hydrochloride by Alternanthera philoxeroides biomass derived porous carbon materials treated with hydrogen peroxide. *RSC Adv.* **2016**, *6*, 79275–79284. [CrossRef]
35. Wei, X.; Fan, Y.; Bi, C.; Yan, X.; Zhang, X.; Li, X. Crystal Structure and Tautomerism Study of the Mono-protonated Metformin Salt. *Bull. Korean Chem. Soc.* **2014**, *35*, 3495–3501. [CrossRef]
36. Desai, D.; Wong, B.; Huang, Y.; Ye, Q.; Tang, D.; Guo, H.; Huang, M.; Timmins, P. Surfactant-Mediated Dissolution of Metformin Hydrochloride Tablets: Wetting Effects Versus Ion Pairs Diffusivity. *J. Pharm. Sci.* **2014**, *103*, 920–926. [CrossRef] [PubMed]
37. Decornez, H.; Drukker, K.; Hammes-Schiffer, S. Solvation and Hydrogen-Bonding Effects on Proton Wires. *J. Phys. Chem. A* **1999**, *103*, 2891–2898. [CrossRef]
38. Bharatam, P.V.; Patel, D.S.; Iqbal, P. Pharmacophoric Features of Biguanide Derivatives: An Electronic and Structural Analysis. *J. Med. Chem.* **2005**, *48*, 7615–7622. [CrossRef]
39. Khan, B.A.; Ahmad, M.; Iqbal, S.; Ullah, F.; Bolan, N.; Solaiman, Z.M.; Shafique, M.A.; Siddique, K.H. Adsorption and immobilization performance of pine-cone pristine and engineered biochars for antimony in aqueous solution and military shooting range soil: An integrated novel approach. *Environ. Pollut.* **2023**, *317*, 120723. [CrossRef]
40. Liu, Y.; Gao, Z.; Ji, X.; Wang, Y.; Zhang, Y.; Sun, H.; Li, W.; Wang, L.; Duan, J. Efficient Adsorption of Tebuconazole in Aqueous Solution by Calcium Modified Water Hyacinth-Based Biochar: Adsorption Kinetics, Mechanism, and Feasibility. *Molecules* **2023**, *28*, 3478. [CrossRef]

41. Divine, C.; Killingstad, M.; Mortensen, L.; Beciragic, A.; Dettmer, A.; Alspach, B. The Plastiverse Extends to Hydrogeologic Systems: Microplastics Are an Important Emerging Groundwater Contaminant Class. *Groundw. Monit. Remediat.* **2024**, *44*, 15–38. [CrossRef]
42. Lan, T.; Wang, T.; Cao, F.; Yu, C.; Chu, Q.; Wang, F. A comparative study on the adsorption behavior of pesticides by pristine and aged microplastics from agricultural polyethylene soil films. *Ecotoxicol. Environ. Saf.* **2021**, *209*, 111781. [CrossRef]
43. Wang, J.; Liu, X.; Liu, G. Sorption behaviors of phenanthrene, nitrobenzene, and naphthalene on mesoplastics and microplastics. *Environ. Sci. Pollut. Res.* **2019**, *26*, 12563–12573. [CrossRef]
44. Li, J.; Zhang, K.; Zhang, H. Adsorption of antibiotics on microplastics. *Environ. Pollut.* **2018**, *237*, 460–467. [CrossRef] [PubMed]
45. Zhao, M.; Huang, L.; Arulmani, S.R.B.; Yan, J.; Wu, L.; Wu, T.; Zhang, H.; Xiao, T. Adsorption of Different Pollutants by Using Microplastic with Different Influencing Factors and Mechanisms in Wastewater: A Review. *Nanomaterials* **2022**, *12*, 2256. [CrossRef] [PubMed]
46. Garrido-López, Á.; Esquiu, V.; Tena, M.T. Comparison of three gas chromatography methods for the determination of slip agents in polyethylene films. *J. Chromatogr. A* **2007**, *1150*, 178–182. [CrossRef] [PubMed]
47. Lv, M.; Zhang, T.; Ya, H.; Xing, Y.; Wang, X.; Jiang, B. Effects of heavy metals on the adsorption of ciprofloxacin on polyethylene microplastics: Mechanism and toxicity evaluation. *Chemosphere* **2023**, *315*, 137745. [CrossRef] [PubMed]
48. Guo, X.; Wang, J. Sorption of antibiotics onto aged microplastics in freshwater and seawater. *Mar. Pollut. Bull.* **2019**, *149*, 110511. [CrossRef] [PubMed]
49. Kalumpha, M.; Guyo, U.; Zinyama, N.P.; Vakira, F.M.; Nyamunda, B.C. Adsorptive potential of *Zea mays* tassel activated carbon towards the removal of metformin hydrochloride from pharmaceutical effluent. *Int. J. Phytoremediat.* **2019**, *22*, 148–156. [CrossRef]
50. Lim, C.; Kim, N.; Lee, J.; Yoon, Y. Potential of Adsorption of Diverse Environmental Contaminants onto Microplastics. *Water* **2022**, *14*, 4086. [CrossRef]
51. Chen, X.; Gu, X.; Bao, L.; Ma, S.; Mu, Y. Comparison of adsorption and desorption of triclosan between microplastics and soil particles. *Chemosphere* **2021**, *263*, 127947. [CrossRef]
52. Guo, C.; Wang, L.; Lang, D.; Qian, Q.; Wang, W.; Wu, R.; Wang, J. UV and chemical aging alter the adsorption behavior of microplastics for tetracycline. *Environ. Pollut.* **2023**, *318*, 120859. [CrossRef]
53. Bao, Z.-Z.; Chen, Z.-F.; Zhong, Y.; Wang, G.; Qi, Z.; Cai, Z. Adsorption of phenanthrene and its monohydroxy derivatives on polyvinyl chloride microplastics in aqueous solution: Model fitting and mechanism analysis. *Sci. Total. Environ.* **2021**, *764*, 142889. [CrossRef]
54. Lu, J.; Wu, J.; Wu, J.; Zhang, C.; Luo, Y. Adsorption and Desorption of Steroid Hormones by Microplastics in Seawater. *Bull. Environ. Contam. Toxicol.* **2021**, *107*, 730–735. [CrossRef] [PubMed]
55. Obayomi, K.S.; Lau, S.Y.; Akubuo-Casmir, D.; Yahya, M.D.; Auta, M.; Bari, A.F.; Oluwadiya, A.E.; Obayomi, O.V.; Rahman, M.M. Adsorption of endocrine disruptive congo red onto biosynthesized silver nanoparticles loaded on Hildegardia barteri activated carbon. *J. Mol. Liq.* **2022**, *352*, 118735. [CrossRef]
56. Chen, S.; Tan, Z.; Qi, Y.; Ouyang, C. Sorption of tri-n-butyl phosphate and tris(2-chloroethyl) phosphate on polyethylene and polyvinyl chloride microplastics in seawater. *Mar. Pollut. Bull.* **2019**, *149*, 110490. [CrossRef] [PubMed]
57. Wang, Y.; Luo, J.; Qin, J.; Huang, Y.; Ke, T.; Luo, Y.; Yang, M. Efficient removal of phytochrome using rice straw-derived biochar: Adsorption performance, mechanisms, and practical applications. *Bioresour. Technol.* **2023**, *376*, 128918. [CrossRef]
58. Huang, H.; Zheng, Y.; Wei, D.; Yang, G.; Peng, X.; Fan, L.; Luo, L.; Zhou, Y. Efficient removal of pefloxacin from aqueous solution by acid–alkali modified sludge-based biochar: Adsorption kinetics, isotherm, thermodynamics, and mechanism. *Environ. Sci. Pollut. Res.* **2022**, *29*, 43201–43211. [CrossRef]
59. McDougall, L.; Thomson, L.; Brand, S.; Wagstaff, A.; Lawton, L.A.; Petrie, B. Adsorption of a diverse range of pharmaceuticals to polyethylene microplastics in wastewater and their desorption in environmental matrices. *Sci. Total. Environ.* **2022**, *808*, 152071. [CrossRef]
60. Wu, P.; Tang, Y.; Jin, H.; Song, Y.; Liu, Y.; Cai, Z. Consequential fate of bisphenol-attached PVC microplastics in water and simulated intestinal fluids. *Environ. Sci. Ecotechnol.* **2020**, *2*, 100027. [CrossRef]